HOLOGIC®
The Science of Sure

Powerful images.
Clear answers.

Manage Patient's concerns about Atypical Femur Fracture*

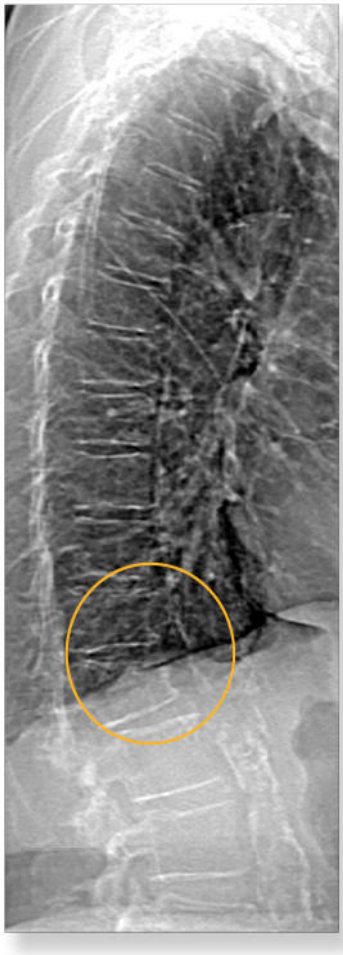

Vertebral Fracture Assessment – a critical part of a complete fracture risk assessment

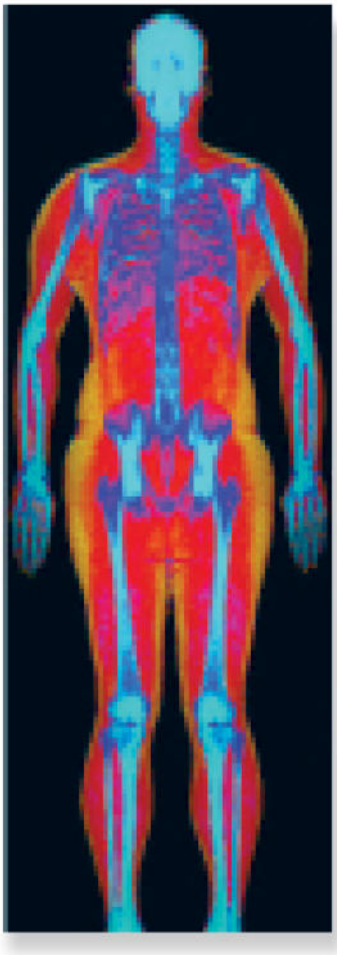

Advanced Body Composition® Assessment – the power to see what's inside

Contact your Hologic rep today at BSHSalesSupportUS@hologic.com

*Incomplete Atypical Femur Fractures imaged with a Hologic densitometer, courtesy of Prof. Cheung, University of Toronto

www.hologic.com | dxaperformance.com | 1.800.442.9892

LIGHT/TNFSF14 promotes osteolytic bone metastases in non-small cell lung cancer patients

Giacomina Brunetti [1], Dimas C. Belisario [2], Sara Bortolotti [3], Giuseppina Storlino [3], Graziana Colaianni [3], Maria Felicia Faienza [4], Lorenzo Sanesi [3], Valentina Alliod [5], Lucio Buffoni [5], Elisa Centini [2], Claudia Voena [2, 6], Roberta Pulito [2], Silvia Novello [6], Giuseppe Ingravallo [7], Rita Rizzi,[7] Giorgio Mori[8], Janne E Reseland,[9] Carl F. Ware [10], Silvia Colucci [1], Riccardo Ferracini [11], Maria Grano [3*] and Ilaria Roato [2*]

[1] Department of Basic and Medical Sciences, Neurosciences and Sense Organs, section of Human Anatomy and Histology, University of Bari, Bari, Italy; [2] Center for Experimental Research and Medical Studies (CeRMS), A.O.U. Città della Salute e della Scienza di Torino, Turin, Italy; [3] Department of Emergency and Organ Transplantation, section of Human Anatomy and Histology, University of Bari, Bari, Italy; [4] Department of Biomedical Science and Human Oncology, University of Bari, Bari, Italy; [5] Department of Oncological Sciences, University of Turin Medical School, Turin, Italy; [6] Department of Molecular Biotechnology and Health Sciences, University of Turin, Turin, Italy; [7] Department of Emergency and Organ Transplantation, University of Bari, Bari, Italy; [8] Department of Clinical and Experimental Medicine, University of Foggia, Foggia, Italy; [9] Department of Biomaterials, Institute for Clinical Dentistry, University of Oslo, Blindern, Oslo, Norway; [10] Infectious and Inflammatory Disease Center, Sanford Burnham Prebys Medical Discovery Institute, La Jolla, CA, USA; [11] Department of Surgical Sciences (DISC), Orthopaedic Clinic-IRCCS, A.O.U. San Martino, Genoa, Italy

* Equally contributed

Corresponding Author:
Giacomina Brunetti, PhD
Department of Basic and Medical Sciences, Neurosciences and Sense Organs, section of Human Anatomy and Histology, University of Bari,
Piazza Giulio Cesare, 11, 70124 Bari, Italy;
e-mail: giacomina.brunetti@uniba.it
Phone: +39 0805478306; Fax: +39 0805478308

This article has been accepted for publication and undergone full peer review but has not been through the copyediting, typesetting, pagination and proofreading process which may lead to differences between this version and the Version of Record. Please cite this article as doi: 10.1002/jbmr.3942

ABSTRACT

Tumor necrosis factor superfamily member 14 (*TNFSF14*), LIGHT, is a component of the cytokine network that regulates innate and adaptive immune responses, which promote homeostasis of lymphoid organs, liver, and bone. Metastatic tumors often disrupt the tissue microenvironment, thus altering the homeostasis of the invaded organ; however, the underlying mechanisms required further studies. We investigated the role of LIGHT in osteolytic bone disease induced by metastatic non-small cell lung cancer (NSCLC). Patients diagnosed with NSCLC bone metastasis show significantly higher levels of LIGHT expressed in monocytes compared with non-bone metastatic tumors and healthy controls. Serum LIGHT levels were also higher in patients with bone metastases than in controls, suggesting a role for LIGHT in stimulating osteoclast precursors. In bone metastatic patients, we also detected increased RNA expression and serum RANKL levels, thus by adding anti-LIGHT or RANK-Fc in PBMC cultures, a significant inhibition of osteoclastogenesis was observed. To model in mice this observation, we used the mouse lung cancer cell line LLC-1. After intratibial implantation, wild-type mice showed an increased number of osteoclasts but reduced numbers of osteoblasts and decreased osteoid formation. In contrast, *Tnfsf14*$^{-/-}$ mice showed no significant bone loss or other changes in bone homeostasis associated with this model. These data indicate LIGHT as a key control mechanism for regulating bone homeostasis during metastatic invasion. Thus, LIGHT may be a novel therapeutic target in osteolytic bone metastases.

Keywords: bone metastasis, osteoclast, LIGHT (*TNFSF14*), non-small cell lung cancer (NSCLC)

INTRODUCTION

Lung cancer represents the primary cause of cancer-related mortality worldwide (1). The predominant form of lung cancer is non-small cell lung cancer (NSCLC), which metastasizes to bone in 30-40% of patients, resulting in a very poor prognosis and median survival time measured in months following lesion detection (2). NSCLC bone metastases are mainly osteolytic and dramatically impact patients' quality of life, causing morbidity and having substantial financial implications for healthcare providers (3). In order to develop innovative strategies to inhibit metastatic tumors, we need to identify molecules which regulate bone metastasis. Cancer stem cells revealed to play an important role in initiating the metastatic process (4) due to their interaction with bone microenvironment and immune system (5). Indeed, the role of the immune system in promoting NSCLC bone metastases has been previously reported (6). Among the immune mediators of bone metastases, the immunostimulatory cytokine, LIGHT, a member of TNF superfamily (*TNFSF14*), may be relevant (7,8). LIGHT is homologous to lymphotoxins and engages the herpes virus entry mediator (HVEM) and the Lymphotoxin-β receptor. LIGHT is produced by immune cells, particularly by activated T-cells, monocytes, natural killers, and neutrophils. It has been reported that LIGHT is involved in increased bone resorption activity typical of the bone diseases, such as erosive rheumatoid arthritis (RA) and multiple myeloma (9). LIGHT synergizes with RANKL to stimulate osteoclastogenesis (10-12) and alternately inhibits osteoblastogenesis in myeloma (12), thus suggesting that high LIGHT levels are harmful for bone. Recently, a study using mice genetically deficient in LIGHT (*Tnfsf14*$^{-/-}$) has showed cancellous bone loss, indicating that LIGHT mediates bone homeostasis (13). Additional evidences have demonstrated that LIGHT expression in T- and B-cell impacts bone homeostasis through the reduced expression of OPG with consequent increased osteoclastogenesis, thus identifying a mechanism that contributes to the interplay between bone and the immune system (13). Given this

evidence in bone homeostasis, we investigated LIGHT in the malignant bone invasion induced by NSCLC.

MATERIALS AND METHODS

Patients. Peripheral Blood (PB) samples were obtained from 61 NSCLC newly diagnosed patients (37 without bone metastases and 24 with bone metastases) and 13 healthy donors. The patient's characteristics are reported in Supplementary Table 1. Patients signed informed consent according to the Declaration of Helsinki and were approved by the Comitato Etico Interaziendale of A.O.U. Città della Salute e della Scienza di Torino – A.O. Ordine Mauriziano -A.S.L. TO1 and of A.O.U. San Luigi Gonzaga di Orbassano.

Flow cytometry analysis. Peripheral Blood Mononuclear Cells (PBMCs) were isolated from PB samples and were stained with the following conjugated antibodies: PE Light (R&D Systems), FITC-CD14 (Millipore), FITC-CD25, APC-CD4 (Caltag), APC-CD8 (GenWay), PerCP-CD16 (Biolegend). Unstained samples and isotypic control antibodies PE, FITC, APC and PerCP-Mouse IgG1, PE-IgG2a (Biolegend and Miltenyi Biotech) were used as negative controls. Samples were analyzed by flow cytometry with FACs Calibur (Becton Dickinson) and Flowlogic software (Miltenyi Biotec).

Osteoclastogenesis. PBMCs were isolated after centrifugation over a density gradient using the Ficoll method. PBMCs were plated in 96-well plates at $5x10^5$ cell/well, using Alpha-Minimal Essential Medium (α-MEM, supplied by Invitrogen), supplemented with 10% fetal bovine serum, benzylpenicillin (100 IU/ml) and streptomycin (100 mg/ml) (Lonza) and maintained at 37°C in a humidified atmosphere of 5% CO_2. To obtain fully differentiated human osteoclasts (OCs), PBMCs from patients with non-bone metastases were cultured in the presence or absence of recombinant human M-CSF (25 ng/ml) and RANKL (30 ng/ml, PeproTech) for 15 days. PBMCs from patients with bone metastases were maintained in α-MEM without any factors, since they spontaneously

differentiated into OCs, as previously described (14). A neutralizing anti-LIGHT mAb (R&D Systems Inc., Minneapolis, MN) was added in cultures at 100 and 500 ng/ml twice weekly. PBMCs were cultured in 96-well plates (5×10^5 cells/well) in the presence of RANK-Fc at 20 ng/ml (PeproTech). At the end of the culture period, cells were stained for tartrate-resistant acid phosphatase (TRAP, kit was supplied by Sigma-Aldrich) and OCs were identified as TRAP-positive multinucleated cells containing three or more nuclei.

Osteoblastogenesis. Primary human mesenchymal stem cells (MSCs) from human exfoliated deciduous teeth (SHED), were obtained according to the procedure previously published (15). Cells were seeded in 24-well-plates at 400/well, cultured alone or in co-cultures with PBMCs ($5.5\ x10^5$ cell/well) in osteogenic differentiating medium, in the absence or presence of 100 ng/ml anti-LIGHT mAb. At the end of culture period (14 days), alkaline phosphatase (ALP) staining (ALP, kit was supplied by Sigma-Aldrich) was performed and the ALP positive colony-forming units (CFU-OB) were counted, as well as the relative percentage of CFU-OB to the total culture area.

Real-Time analysis. Total RNA was extracted by Trizol system (Invitrogen) from patients' PBMC samples, and 1ug of RNA was converted into single-stranded cDNA using the High-Capacity cDNA Reverse Transcription Kit (Applied Biosystems). Quantitative real-time PCR was carried out using SsoAdvanced Universal SYBR Green Supermix and CFX96 system (Bio-Rad). The mRNA expression of DcR3, LTβR, HVEM, OPG and RANKL was evaluated. The β-Actin gene was used as the reference gene. Sequences of the probes and primers were previously published (16).

ELISA. Patients' sera were evaluated for the presence of circulating LIGHT, OPG (R&D Systems), and RANKL (BioVendor), according to the manufacturer's instructions. The results were expressed as mean ± SD.

Retrovirus preparation and cell transduction. Retroviruses were generated by transfecting the Pallino vector expressing green fluorescent protein (GFP) in the 293GP packaging cell line (Invitrogen). Transfected cells were incubated at 37^o C, and supernatants containing viral particles were collected after 24 and 48 hours. For retroviral transduction, 300µl filtered retroviral

supernatants were used to transduce 10 x 10^4 ($1x10^5$) mouse Lewis lung carcinoma cell lines (LLC-1, purchased from CLS, Germany) plated on 6-well plates along with polybrene (8 μg/ml). After 12 hours of incubation, 1 mL complete medium was added, and cells were cultured for additional 48 hours. Transduced cells were then analyzed for GFP expression using a FACSCalibur flow cytometer (Becton Dickinson). The CELLQuest software (Becton Dickinson) was used for data acquisition and analysis.

Immunohistochemistry and histological analysis on human bone biopsies. Immunohistochemistry was performed on 14 patients' NSCLC bone biopsies fixed in 10% neutral buffered formalin and decalcified with EDTA. These samples were kindly provided by Prof. Papotti from the archive of the Department of Pathology of Città della Salute e della Scienza di Torino. Tissues were embedded in paraffin, and sections were deparaffinized, rehydrated through graded alcohols, and subjected to antigen retrieval for immunohistochemistry. Sections were stained for H&E and polyclonal anti-human LIGHT (Sigma-Aldrich, cat.n. HPA012700).

Mouse model. *Tnfsf14* heterozygous mice were kindly provided by Prof Carl F Ware. GFP-conjugated LLC1 (LLC1-GFP) cells were injected intratibially in 6-week-old, female WT and *Tnfsf14*-/- mice. In detail, mice were anesthetized, and 1×10^4 LLC1-GFP cells in 50 μL PBS were injected into the right tibia. PBS (50 μL) was injected into the left tibia for an internal control, as reported in literature (17). 4 to 5 animals were housed in single cage at 23°C on a light/dark cycle and were fed a standard rodent chow. After 14 days mice were euthanized and their tissues were surgically excised. Tibiae were fixed with 4% (vol/vol) paraformaldehyde for 18 hours at 4°C and processed for microCT and histological analysis. This animal interventional study is in accordance with the European Law Implementation of Directive 2010/63/EU and all experimental protocols were reviewed and approved by the Veterinary Department of the Italian Ministry of Health.

Microcomputed tomography analysis of tibiae. MicroCT scanning was used to measure morphological indices of metaphyseal tibia regions. Tibiae were rotated around their long axes, and images were acquired using Bruker Skyscan 1172 (Kontich, Belgium) with the following

parameters: pixel size = 5 μm; peak tube potential = 59kV; X-ray intensity = 167 μA; 0.4° rotation step. A set of 3 hydroxyapatite (HA) phantoms were scanned and used for calibration to compute volumetric BMD. For cortical bone properties, tibiae were scanned at the mid-diaphysis starting 5.5 mm from proximal tibial condyles and extending for 200 6-μm slices (1.2 mm). For trabecular bone, tibiae were scanned starting at 1.9 mm from the proximal tibial condyles, just distal to the growth plate, in the direction of the metaphysis, and extending for 200 slices (1.2 mm).

Histological analysis. For the evaluation of the tumor burden, mouse tibiae were decalcified and embedded with paraffin. Section were stained with hematoxylin-eosin and tumor burden was evaluated as the ratio of tumor area on total area. Microphotographs were captured under a microscope (Leica) using a 10X objective lens and analyzed using ImageJ software.

For bone histomorphometry, tibiae were embedded with methylmethacrylate (MMA) and cut by a standard microtome (RM 2155 Leica, Heidelberg, Germany) into 5-μm slices for histology as previously described (13). For analysis of osteoclasts (OC number per bone perimeter, N.Oc/B.Pm), bone sections were incubated in TRAP staining solution and then counterstained with methyl green; for osteoblast analysis (OB number per bone perimeter, N.Ob/B.Pm), bone sections were stained with toluidine blue. Goldner's Masson trichrome stain was used to analyze new osteoid formation. Microphotographs were captured under a microscope (Leica) using a 40X objective lens and analyzed using ImageJ software**.**

Statistical analyses. Statistical analyses were performed by Student's T-test, non-parametric tests (Mann-Whitney for not normal data), or ANOVA, according to the Statistical Package for the Social Sciences (IBM SPSS) software. Results were considered statistically significant at $p< 0.05$.

RESULTS

Increased LIGHT expression in monocytes and serum from patients with NSCLC bone metastases. Through flow cytometry, we analysed LIGHT expression in CD4 and CD8 T cells, CD14 monocytes, and CD16 neutrophils from 58 out of 61 NSCLC patients enrolled in the study:

22 patients with and 36 without bone metastases, and 13 healthy donors. A significantly higher expression of LIGHT was detectable in monocytes from bone metastatic patients compared with non-bone metastatic NSCLC and healthy donors. (Fig. 1A-C). LIGHT expression by monocytes was higher in patients with metastatic bone lesions than in non-bone metastatic ones (66.5 ± 24.5 vs 43.3 ± 25.2 p = 0.001), healthy donors (66.5 ± 24.5 vs 8.5 ± 4.6 p = 0.0002) and in non-bone metastatic patients than in healthy donors (43.3 ± 25.2 vs 8.5 ± 4.6, p = 0.0001) Fig. 1D. Activated CD4/CD25 T cells express higher levels of LIGHT compared to CD8 T cells but were similar across all groups; no differences were evident among the other cellular subsets. The mean values of LIGHT expression among the different PBMC subpopulations is reported in Supplementary Table 2. Serum LIGHT levels were also significantly higher in bone metastatic patients than in non-bone metastatic ones (186.8 ± 191.2 pg/ml vs 115.8 ± 73 pg/ml, p = 0.04) and healthy donors (186.8 ± 191.2 pg/ml vs 85.7 ± 38.4 pg/ml, p = 0.04) (Fig. 1E). Since LIGHT action is mediated by the interaction with its receptors, LTβR, HVEM and DcR3, we also evaluated their expression on patients' PBMCs. LTβR resulted not expressed, while HVEM and DcR3 expression was not significantly different between bone and non-bone metastatic patients (data not shown).

LIGHT expression in NSCLC bone metastases. In our series of bone metastasis, careful routine histopathological analysis showed atypical epithelial neoplastic cells morphologically consistent with NSCLC within hematopoietic tissue, without evident malignant phenotype. In particular, we investigated the expression of LIGHT in 14 NSCLC metastatic bone biopsies by immunostaining. We found 8 out of 14 tumor epithelial cell cases expressed LIGHT, regardless the absence (Fig. 2A; i.e., early phase of bone marrow colonization) or presence of a reactive background, such as fibrous tissue (Fig. 2B) and osteosclerosis (Fig. 2C). Outstandingly, cytoplasmic staining of LIGHT was intermediate or strong in bone metastases with no gland forming (i.e., solid) NSCLCs, while it was minimal or negative in NSCLCs associated with a gland-forming component (Fig. 2D). The LIGHT expression was not detected in hematopoietic tissue.

LIGHT blockade inhibits osteoclastogenesis *in vitro.* As previously described (6,14), OCs formed spontaneously in PBMC cultures from bone metastatic patients, whereas cells from non-bone metastatic patients required M-CSF and RANKL. The number of OCs in cultures from patients with bone metastases was significantly higher than those from non-bone metastatic cultures, even though these ones received stimulating factors (272 ± 98; 131 ± 49, $p = 0.002$), (Fig. 3A). A neutralizing mAb to LIGHT added to OC cultures of both bone and non-bone metastases inhibited osteoclastogenesis, but the decrease was statistically significant only for bone metastatic patients (272 ± 98 vs 132 ± 74, $p = 0.01$) (Fig. 3B). The significant inhibition of osteoclastogenesis in bone metastatic patients was also confirmed by TRAP staining (Fig. 3B). In PBMCs cultures from non-bone metastases, osteoclastogenesis was only slightly reduced. Indeed, in these patients, LIGHT expression was less than in bone metastatic patients, suggesting that only high level of LIGHT can affect osteoclastogenesis *in vitro*.

RANKL and OPG in NSCLC patients. LIGHT synergises with RANKL to induce osteoclastogenesis (9,12), and spontaneous osteoclastogenesis in bone metastatic patients is regulated by RANKL (6,14). The detection of higher LIGHT expression in patients with bone metastases, suggests that the effect of LIGHT on osteoclastogenesis might be due to a contribution from RANKL. We found serum RANKL levels significantly higher in these patients than in non-bone metastatic ones (17.6 ± 21.2 ng/ml vs 6.5 ± 2.8 ng/ml, respectively). By contrast, serum OPG levels were the same between the two groups (2 ± 0.8 ng/ml vs 1.9 ± 0.6 ng/ml, respectively). However, the RANKL/OPG ratio significantly increased in patients with bone metastases compared to non-bone ones (8.9 ± 10 ng/ml vs 6.8 ± 7.2 ng/ml, respectively $p = 0.04$, Fig. 3C). After analysing RANKL and OPG mRNA expression in PBMCs, we found the same trend as for serum levels, but the difference was not statistically significant (1.2 ± 0.4 vs 0.9 ± 0.3, respectively, Fig. 3D). The significant RANKL increase in patients with bone compared to non-bone metastases

prompted us to test RANK-Fc on PBMCs cultures from bone metastatic patients to demonstrate its ability to inhibit OC formation (Fig. 3E), thus suggesting RANKL involvement in osteoclastogenesis.

Blockade of LIGHT does not affect osteoblastogenesis. We investigated whether LIGHT mediates osteoblastogenesis in co-cultures stimulated by NSCLC PBMCs, since it revealed to be able to inhibit CFU-OB formation in multiple myeloma (12). While PBMCs stimulate MSC proliferation, LIGHT released by PBMC could interfere with CFU-OB, so we added anti-LIGHT to counteract this potential inhibition. We performed co-cultures of SHED-MSCs with PBMCs from patients with both bone and non-bone metastases in osteogenic medium, with or without 100ng/ml of anti-LIGHT mAb (Fig. 4). Anti-LIGHT did not affect CFU-OB formation in co-cultures of patients with non-bone or bone metastases, as shown by alkaline phosphatase staining (Fig.4A and 4B, respectively). We observed decreased CFU-OB formation in patients with bone metastases compared to non-bone metastases, even though the difference was not statistically significant (Fig. 4C). These data support the known defect in OB formation and activity in the presence of osteolytic bone metastases.

***Tnfsf14*$^{-/-}$ mice injected with LLC1 are protected from bone loss.** To evaluate *in vivo* the effect of LIGHT neutralization, we injected intratibial WT and *Tnfsf14*$^{-/-}$ (KO) mice with the murine Lewis lung cancer cell line LLC-1. Interestingly, in tibiae the tumor burden, measured by histologic analysis, showed a slight reduction of tumor area in KO bones respect to WT-mice (Fig 5). Furthermore, quantitative observations of microCT generated section images of tibiae (Fig. 6) showing a significant decrease in trabecular bone mass in WT-injected mice compared to the WT-vehicle (Fig. 6A-B). Interestingly, no significant differences were observed between KO-injected mice and the KO-vehicle (Fig. 6C-D), as well as for WT-injected vs KO-injected mice (Fig.6B-D), notwithstanding a reduction trend. In particular, the injected WT mice showed significantly reduced

BV/TV, Tb.N, Tb.Th, and Tb.Sp compared to the WT-vehicle (E-H). Otherwise, these parameters did not show significant variation in KO-injected mice towards the vehicle or in WT-injected mice vs KO-injected mice. We consistently found a significant increase in TRAP-stained OC number per bone perimeter observed only in WT-injected mice vs the WT-vehicle (Fig. 7A). Significantly, slight decrease in OB cell numbers was measured in WT-injected mice compared to WT-vehicle (Fig. 7B). Otherwise, there were no significant differences between KO-injected and vehicle mice as well as for WT- and KO-injected mice (Fig. 7B). Furthermore, a ~52% reduction in the area of osteoid surface to bone surface (OS/BS) was observed in WT-injected mice compared to the WT vehicle ($p < 0.001$), whereas in KO-injected mice, a slight OS/BS% decrease was observed, not statistically significant compared to the KO-vehicle (Fig. 7C). OS/BS% detected between WT- and KO-injected mice did not show any significant difference (Fig. 7C). Overall, our data suggest that LIGHT deficiency protects the loss of bone associated with LLC1 tumor cells.

DISCUSSION

In this study, we demonstrated for the first time that, in patients with bone metastases from NSCLC, LIGHT expression increased in circulating monocytes compared to patients without bone metastases. Previously, it was reported that multiple myeloma patients with bone disease showed an increased expression of LIGHT in both CD14+ monocytes and CD16+ neutrophils (12) together with the role played by LIGHT in regulating osteoclastogenesis. Both NSCLC and multiple myeloma are characterized by osteolytic bone disease, so increased LIGHT expression from monocytes (which can differentiate into OCs) suggests that LIGHT is also involved in the pathogenesis of osteolytic bone metastases from NSCLC. During the analysis of LIGHT expression in CD4+ and CD8+ T cells, as well as CD16+ neutrophils, we found out higher expression in CD4/CD25+ cells than CD8+ T cells, although no difference was seen between bone and non-bone metastatic patients. This suggests that LIGHT expressed in CD4 T cells could stimulate OC

formation, as well as other factors (i.e., IL-7, RANKL, TNF) released by CD4 T cells, known to promote osteoclastogenesis (18,19).

LIGHT production is reflected in the serum concentration; indeed, it was significantly increased in NSCLC bone metastatic patients, suggesting that LIGHT might regulate systemic osteolysis by activating circulating OC precursors.

NSCLC bone biopsies showed distinctive LIGHT expression in bone metastases. Specifically, the LIGHT staining in the samples was markedly associated with less-differentiated cancer cells, while only minimal or negative expression was detected where intraosseous neoplastic cells were organized in a gland-forming pattern, this being considered a histopathological detail of non-aggressive behavior. This pattern of staining could reflect the association of LIGHT bound to Decoy Receptor-3, a soluble receptor that binds LIGHT, present in bone and other tissues, and secreted by tumor cells (20). Consequently, we advocated a new perspective in studying the role of LIGHT in NSCLC cells by considering their differentiation status. In fact, as previously reported with reference to a model of colon cancer, enforced LIGHT expression in tumor cells triggered regression of established tumors and slowed metastatic formation due to LIGHT stimulating an anti-tumor response (21,22). Our finding about the variation of LIGHT expression, according to the differentiated status of NSCLC cells, leads us to speculate that NSCLC cells may use a different ability to escape the immune system.

We also confirm the role of LIGHT in sustaining OC formation using an *in vitro* osteoclastogenesis assay based on patients' PBMC cultures. Specifically, a neutralizing anti-LIGHT antibody inhibited osteoclastogenesis in PBMCs of patients with bone metastases, whereas in PBMC cultures from patients with non-bone metastases, osteoclastogenesis was only slightly reduced. These results suggest that patients without bone metastases expressed LIGHT at physiological levels, which did not affect osteoclastogenesis; namely, the anti-LIGHT did not significantly inhibit OC formation. It has been recently demonstrated that, physiologically, LIGHT interfered with bone homeostasis protecting bone, while the absence of LIGHT caused cancellous bone loss. Truly, LIGHT

deficiency is associated with pro-osteoclastogenic stimulation and increased OC bone resorption (13). To the same degree, elevated LIGHT levels in NSCLC patients can activate osteolytic mechanisms, which is also a function of the RANK/RANKL/OPG axis (6). Here, we show that adding RANK-Fc to PBMC cultures significantly inhibited osteoclastogenesis in NSCLC patients with bone metastases, suggesting that both RANKL and LIGHT contribute to bone disease.

In basal conditions, osteoclastogenesis is mainly regulated by RANKL/OPG ratio. Here, in our cohort of NSCLC bone metastatic patients, we observed high LIGHT levels and an unbalanced RANKL/OPG ratio in favour of RANKL. Indeed, patients with bones metastases had higher levels of RANKL than non-bone metastatic ones, whereas OPG levels were comparable between the two groups. LIGHT-KO mice also showed an unbalanced RANKL/OPG ratio, due to OPG variations, while RANKL levels did not differ (13). In patients with osteolytic bone disease as well as in Multiple Myeloma patients previously shown (23), we detected both high levels of RANKL and LIGHT, which up-regulated osteoclastogenesis. Conversely, in *Tnfsf14*-/- mice, OPG increased, but the result was always an unbalanced RANKL/OPG ratio associated with an up-regulation of osteoclastogenesis (13). These data corroborate a fundamental role of LIGHT in the maintenance of skeletal physiology, since its dysregulation causes abnormal osteoclastogenesis.

In order to study the potential effects of LIGHT on osteoblastogenesis, we co-cultured SHED-derived MSCs and patients PBMCs in the presence or absence of anti-LIGHT antibody. By contrast to LIGHT KO mice and multiple myeloma, we observed no significant LIGHT effect on osteoblastogenesis. We also found out a decreased CFU-OB formation in patients with bone metastases compared to non-bone ones. Despite this difference not statistically significant, the results support the known defect in OB formation and activity in the presence of osteolytic bone metastases (5).

The mouse NSCLC-bone disease model revealed that the tumor burden was reduced in KO bones compared to WT-mice. Furthermore, LIGHT deficiency prevented significant decrease in bone mass, whereas increased osteoclastogenesis and decreased osteoblastogenesis occurred in WT mice.

Osteoid formation was also significantly reduced only in tumor bearing WT mice, while KO mice showed only a slight reduction suggesting a key role for LIGHT to cause bone disease in metastatic patients. In KO-LLC1 injected mice, the reduced bone disease may occur due to the decreased tumor burden compared to WT-injected mice. Nevertheless, we cannot exclude that the absence of further bone loss with tumor injection in KO mice might depend on the already low bone mass, associated to the LIGHT KO phenotype. A similar scenario has been described for another co-stimulatory cytokine, CD40L, indeed mice lacking CD40L do not sustain the acute bone loss triggered by estrogen deficiency (24).

We previously reported that *Tnfsf14*-/- mice showed a reduced trabecular bone mass compared to WT mice as well as high levels of LIGHT in different pathologies with osteolytic bone disease, such as multiple myeloma (12,23), alkaptonuria (25), chronic kidney disease, and hemodialysis in patients (26). Moreover, Edwards et al. measured increased LIGHT levels in erosive rheumatoid arthritis, thus sustaining its central role in pathological bone remodelling.

In conclusion, the accumulated evidence supports a key role of LIGHT in pathological bone remodelling and suggests that neutralizing LIGHT activity could improve bone loss in patients with NSCLC.

Acknowledgments

We thank dr. Federico Mussano and prof. Mauro Papotti for providing us SHED-MSCs and NSCLC bone biopsies, respectively. A special thanks to Dr. Mara Compagno for critical discussion of the manuscript.

This work was supported by the CRT and Compagnia di San Paolo Foundations; Fondazione Ricerca Molinette ONLUS (I.R.).

Authors' roles: GB and IR designed the study, and drafted the manuscript; SB performed histological studies; DCB, EC, and RP: performed experiments on human biologicalsamples; LS performed ELISA, GI performed immunohistochemistry; VA, SN and LB recruited patients,

provided samples and clinical data; CV performed retrovirus preparation and cell transduction; GM performed the statistical analysis; RR and MFF critically revised the clinics; CFW provides mice and critically revised the manuscript; JER provides her expertise in microCT; GC and GS analyzed microCT results; SC and RF critically revised the manuscript; MG supervises all experiments and critically revised the manuscript. All authors read and approved the final manuscript. GB and IR take responsibility for the integrity of the data analysis.

1. Bray F, Ferlay J, Soerjomataram I, Siegel RL, Torre LA, Jemal A. Global cancer statistics 2018: GLOBOCAN estimates of incidence and mortality worldwide for 36 cancers in 185 countries. CA Cancer J Clin 2018;68:394-424
2. Langer CJ, Besse B, Gualberto A, Brambilla E, Soria JC. The evolving role of histology in the management of advanced non-small-cell lung cancer. J Clin Oncol 2010;28:5311-20
3. Delea T, Langer C, McKiernan J, Liss M, Edelsberg J, Brandman J, *et al.* The cost of treatment of skeletal-related events in patients with bone metastases from lung cancer. Oncology 2004;67:390-6
4. Bertolini G, D'Amico L, Moro M, Landoni E, Perego P, Miceli R, *et al.* Microenvironment-Modulated Metastatic CD133+/CXCR4+/EpCAM- Lung Cancer-Initiating Cells Sustain Tumor Dissemination and Correlate with Poor Prognosis. Cancer Res 2015;75:3636-49
5. Roato I, Ferracini R. Cancer Stem Cells, Bone and Tumor Microenvironment: Key Players in Bone Metastases. Cancers (Basel) 2018;10
6. Roato I, Gorassini E, Buffoni L, Lyberis P, Ruffini E, Bonello L, *et al.* Spontaneous osteoclastogenesis is a predictive factor for bone metastases from non-small cell lung cancer. Lung Cancer 2008;61:109-16
7. Mauri DN, Ebner R, Montgomery RI, Kochel KD, Cheung TC, Yu GL, *et al.* LIGHT, a new member of the TNF superfamily, and lymphotoxin alpha are ligands for herpesvirus entry mediator. Immunity 1998;8:21-30
8. Tamada K, Shimozaki K, Chapoval AI, Zhai Y, Su J, Chen SF, *et al.* LIGHT, a TNF-like molecule, costimulates T cell proliferation and is required for dendritic cell-mediated allogeneic T cell response. J Immunol 2000;164:4105-10
9. Edwards JR, Sun SG, Locklin R, Shipman CM, Adamopoulos IE, Athanasou NA, *et al.* LIGHT (TNFSF14), a novel mediator of bone resorption, is elevated in rheumatoid arthritis. Arthritis Rheum 2006;54:1451-62
10. Ishida S, Yamane S, Nakano S, Yanagimoto T, Hanamoto Y, Maeda-Tanimura M, *et al.* The interaction of monocytes with rheumatoid synovial cells is a key step in LIGHT-mediated inflammatory bone destruction. Immunology 2009;128:e315-24
11. Hemingway F, Kashima TG, Knowles HJ, Athanasou NA. Investigation of osteoclastogenic signalling of the RANKL substitute LIGHT. Exp Mol Pathol 2013;94:380-5
12. Brunetti G, Rizzi R, Oranger A, Gigante I, Mori G, Taurino G, *et al.* LIGHT/TNFSF14 increases osteoclastogenesis and decreases osteoblastogenesis in multiple myeloma-bone disease. Oncotarget 2014;5:12950-67
13. Brunetti G, Faienza MF, Colaianni G, Gigante I, Oranger A, Pignataro P, *et al.* Impairment of Bone Remodeling in LIGHT/TNFSF14-Deficient Mice. J Bone Miner Res 2018;33:704-19
14. Roato I, Grano M, Brunetti G, Colucci S, Mussa A, Bertetto O, *et al.* Mechanisms of spontaneous osteoclastogenesis in cancer with bone involvement. FASEB J 2005;19:228-30

15. Mussano F, Genova T, Petrillo S, Roato I, Ferracini R, Munaron L. Osteogenic Differentiation Modulates the Cytokine, Chemokine, and Growth Factor Profile of ASCs and SHED. Int J Mol Sci 2018;19
16. D'Amelio P, Roato I, D'Amico L, Veneziano L, Suman E, Sassi F, *et al.* Bone and bone marrow pro-osteoclastogenic cytokines are up-regulated in osteoporosis fragility fractures. Osteoporos Int 2011;22:2869-77
17. Wright LE, Ottewell PD, Rucci N, Peyruchaud O, Pagnotti GM, Chiechi A, Buijs JT, Sterling JA. Murine models of breast cancer bone metastasis. Bonekey Rep. 2016;5:804.
18. Horwood NJ, Kartsogiannis V, Quinn JM, Romas E, Martin TJ, Gillespie MT. Activated T lymphocytes support osteoclast formation in vitro. Biochem Biophys Res Commun 1999;265:144-50
19. Takayanagi H, Ogasawara K, Hida S, Chiba T, Murata S, Sato K, *et al.* T-cell-mediated regulation of osteoclastogenesis by signalling cross-talk between RANKL and IFN-gamma. Nature 2000;408:600-5
20. Cheung TC, Coppieters K, Sanjo H, Oborne LM, Norris PS, Coddington A, *et al.* Polymorphic variants of LIGHT (TNF superfamily-14) alter receptor avidity and bioavailability. J Immunol 2010;185:1949-58
21. Qiao G, Qin J, Kunda N, Calata JF, Mahmud DL, Gann P, *et al.* LIGHT Elevation Enhances Immune Eradication of Colon Cancer Metastases. Cancer Res 2017;77:1880-91
22. Yu P, Lee Y, Liu W, Chin RK, Wang J, Wang Y, *et al.* Priming of naive T cells inside tumors leads to eradication of established tumors. Nat Immunol 2004;5:141-9
23. Brunetti G, Rizzi R, Storlino G, Bortolotti S, Colaianni G, Sanesi L, *et al.* LIGHT/TNFSF14 as a New Biomarker of Bone Disease in Multiple Myeloma Patients Experiencing Therapeutic Regimens. Front Immunol 2018;9:2459
24. Li JY, Tawfeek H, Bedi B, Yang X, Adams J, Gao KY, Zayzafoon M, Weitzmann MN, Pacifici R. Ovariectomy disregulates osteoblast and osteoclast formation through the T-cell receptor CD40 ligand. Proc Natl Acad Sci U S A. 2011;108(2):768-773.
25. Brunetti G, Tummolo A, D'Amato G, Gaeta A, Ortolani F, Piacente L, *et al.* Mechanisms of Enhanced Osteoclastogenesis in Alkaptonuria. Am J Pathol 2018;188:1059-68
26. Cafiero C, Gigante M, Brunetti G, Simone S, Chaoul N, Oranger A, *et al.* Inflammation induces osteoclast differentiation from peripheral mononuclear cells in chronic kidney disease patients: crosstalk between the immune and bone systems. Nephrol Dial Transplant 2018;33:65-75

Figure legends

Figure 1. LIGHT expression in monocytes and serum from NSCLC patients. Representative dot plots of CD14+/LIGHT+ monocytes from healthy donors and patients without or with bone metastases are shown (A-C, respectively). Significant increase of LIGHT expression on CD14+ cells derived from patients without or with bone metastases compared to healthy donors, and from patients with bone metastases compared to non-bone metastastic ones (D). Increased serum LIGHT levels in patients without and with bone metastases with respect to healthy donors (E). Comparison of multiple means was performed by One-Way ANOVA; *p* values as shown.

Figure 2. LIGHT expression in NSCLC bone metastases. LIGHT detected in tumor epithelial cells, regardless of the absence (A and D) or presence of a reactive background, such as fibrous tissue (B) and osteosclerosis (C). Cytoplasmic staining of LIGHT is minimal or negative in NSCLCs associated with a gland forming component (D). As it can be noticed, in cases A and D it is also clear hematopoietic tissue; while, in cases B and C the carcinomatous infiltration is massive without residual bone marrow. Photomicrographs on the right: original magnification 100X. Photomicrographs on the left: original magnification 200X.

Figure 3. LIGHT and RANKL in the regulation of osteoclastogenesis *in vitro*. Increased number of multinucleated (> 3 nuclei), TRAP positive OCs in bone metastatic patients compared to non-bone metastatic ones, and reduced OC number in bone metastatic patients after anti-LIGHT treatment (500 ng/ml) (A). Comparison of multiple means was performed by One-Way ANOVA. Representative images of TRAP staining for OCs derived from bone metastatic patients (B), in absence (CTRL) or presence of 100 and 500 ng/ml of anti-LIGHT. Increased RANKL/OPG ratio in patients with bone metastases compared to non-bone ones (C); gene expression analysis, reported as RANKL/OPG ratio (D); significant reduction in osteoclastogenesis in PBMC cultures treated with RANK-Fc (20 ng/ml) (E). Two-tailed unpaired *T*- tests were conducted for serum level and gene expression of RANKL/OPG, two-tailed paired *T*-test was conducted for RANK-Fc experiments; *p* values as shown. Magnification 10X.

Figure 4. LIGHT does not affect osteoblastogenesis in co-cultures of SHED-MSCs and patients' PBMCs.

Representative image of ALP staining for CFU-OB in co-cultures of patients without bone (A) and with bone metastases (B), in absence or presence of 100 ng/ml anti-LIGHT neutralizing mAb. The mean number of CFU-OB/total area was not different in presence or absence of anti-LIGHT for both bone and non-bone metastatic patients. (C). Data are derived from cultures of 4 non-bone metastatic patients and 3 bone metastatic ones. Two-tailed paired *T*-tests were performed on both bone and non-bone metastastic groups; *p* values as shown. Magnification 10X.

Figure 5. *Tnfsf14*−/− mice display decreased tumor burden in bone. Representative haematoxylin-eosin stained sections from WT (A) and KO (B) tibiae injected with Lewis lung carcinoma cell lines (LLC-1). Graphs report calculated histologic analysis of tumor area/total bone area for WT and KO-injected mice (C), a slight decrease in tumor area in KO bones respect to WT-mice was evident. Arrows point to tumor cells. The marked area represents the tumor area. N = 10 mice per group. Two-tailed paired *T*-tests were performed; *p* value as shown.

Figure 6. ***Tnfsf14*$^{-/-}$ mice injected with LLC1 are protected from bone loss.** Representative microCT-generated section images of trabecular bone in tibiae harvested from WT and *Tnfsf14*$^{-/-}$ mice, previously injected with vehicle or Lewis lung carcinoma cell lines (LLC-1), A-D. Graphs report calculated trabecular parameters at the metaphysis of WT and *Tnfsf14*$^{-/-}$ mice (E-G). Trabecular bone parameters included bone volume/total volume (BV/TV), trabecular thickness (Tb.Th), trabecular number (Tb.N), and trabecular separation (Tb.Sp). The injected WT mice displayed significantly reduced BV/TV, Tb.N, Tb.Th, and Tb.Sp compared to the WT-vehicle. These parameters did not show significant variation for KO-injected mice with respect to the vehicle or for WT-injected mice vs KO-injected mice. N = 10 mice per group. Comparison of multiple means was performed by One-Way ANOVA; *p* values as shown.

Figure 7. **LIGHT stimulates osteoclastogenesis and inhibits osteoblastogenesis *in vivo*.** Representative images of tartrate-resistant acid phosphatase-stained osteoclasts in tibiae sections from WT and *Tnfsf14*$^{-/-}$ mice, injected with vehicle or Lewis lung carcinoma cell lines (LLC-1), together with OC number per bone perimeter (N.Oc)/B.Pm. A significant increase of OC number was observed only in WT-injected mice compared to the WT-vehicle (A). Toluidine blue-stained osteoblasts in tibial sections from the same mice together with OB number counts per bone perimeter (N.Ob/B.Pm). A slight but significant decrease in OB cell numbers was measured in WT-injected mice compared to WT-vehicle (B). Representative images of Goldner's Masson trichrome-stained vertebral sections, together with measurement of percentage of osteoid per bone surface (BS). A significant reduction was observed only in WT-injected mice compared to the WT vehicle

(C). N = 6 mice per group. Comparison of multiple means was performed by One-Way ANOVA; *p* values as shown. Magnification 40X.

Figure 7. **LIGHT stimulates osteoclastogenesis and inhibits osteoblastogenesis *in vivo*.** Representative images of tartrate-resistant acid phosphatase-stained osteoclasts in tibiae sections from WT and *Tnfsf14*$^{-/-}$ mice, injected with vehicle or Lewis lung carcinoma cell lines (LLC-1), together with OC number per bone perimeter (N.Oc)/B.Pm. A significant increase in OC number was observed only in WT-injected mice with respect to the WT-vehicle (A). Toluidine blue-stained osteoblasts in tibial sections from the same mice together with OB number counts per bone perimeter (N.Ob/B.Pm). A slight but significant decrease in OB cell numbers was measured in WT-injected mice compared with WT-vehicle (B). Representative images of Goldner's Masson trichrome-stained vertebral sections, together with measurement of percentage of osteoid per bone surface (BS). A significant reduction was observed only in WT-injected mice compared to the WT vehicle (C). Statistics: ANOVA, n = 6 mice per group, *p* values as shown. Magnification 40×.

Fig. 1

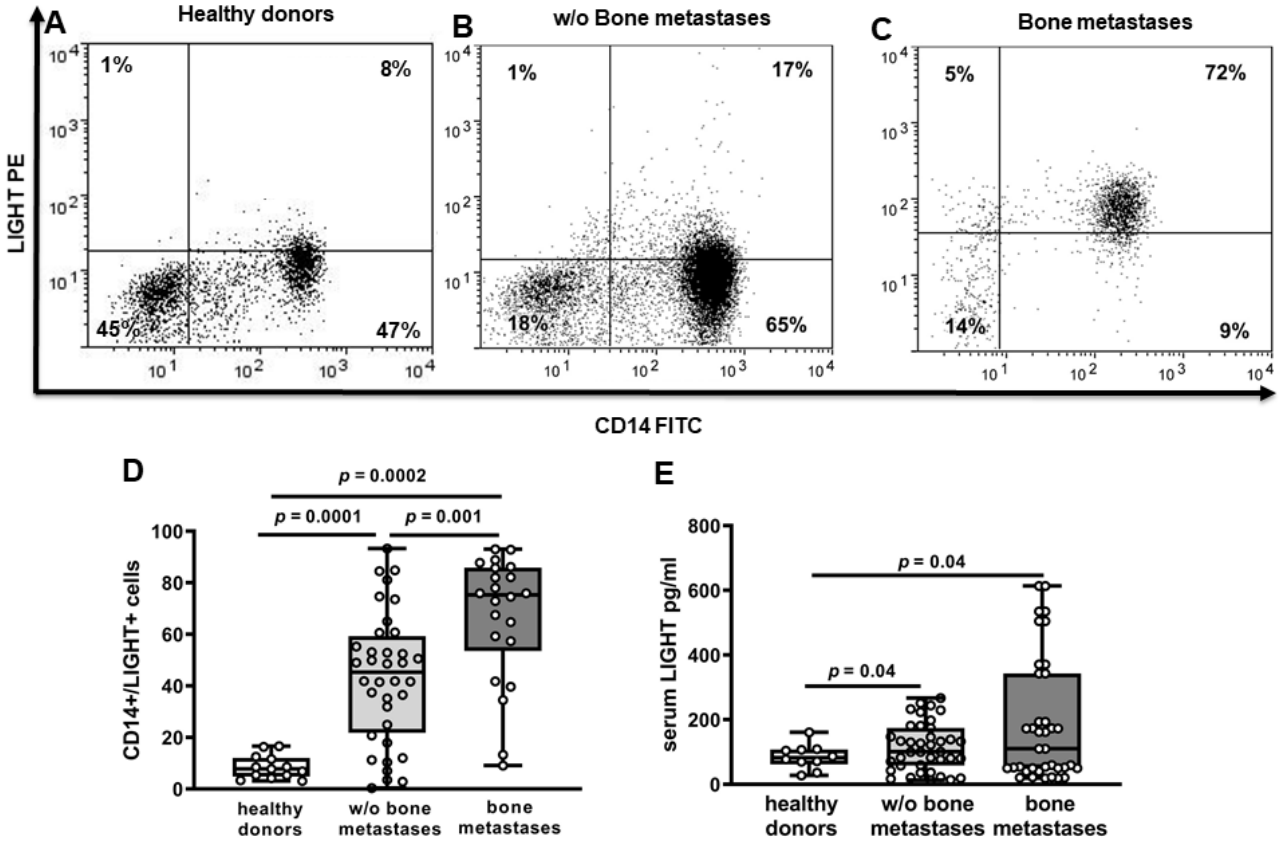

Fig. 2

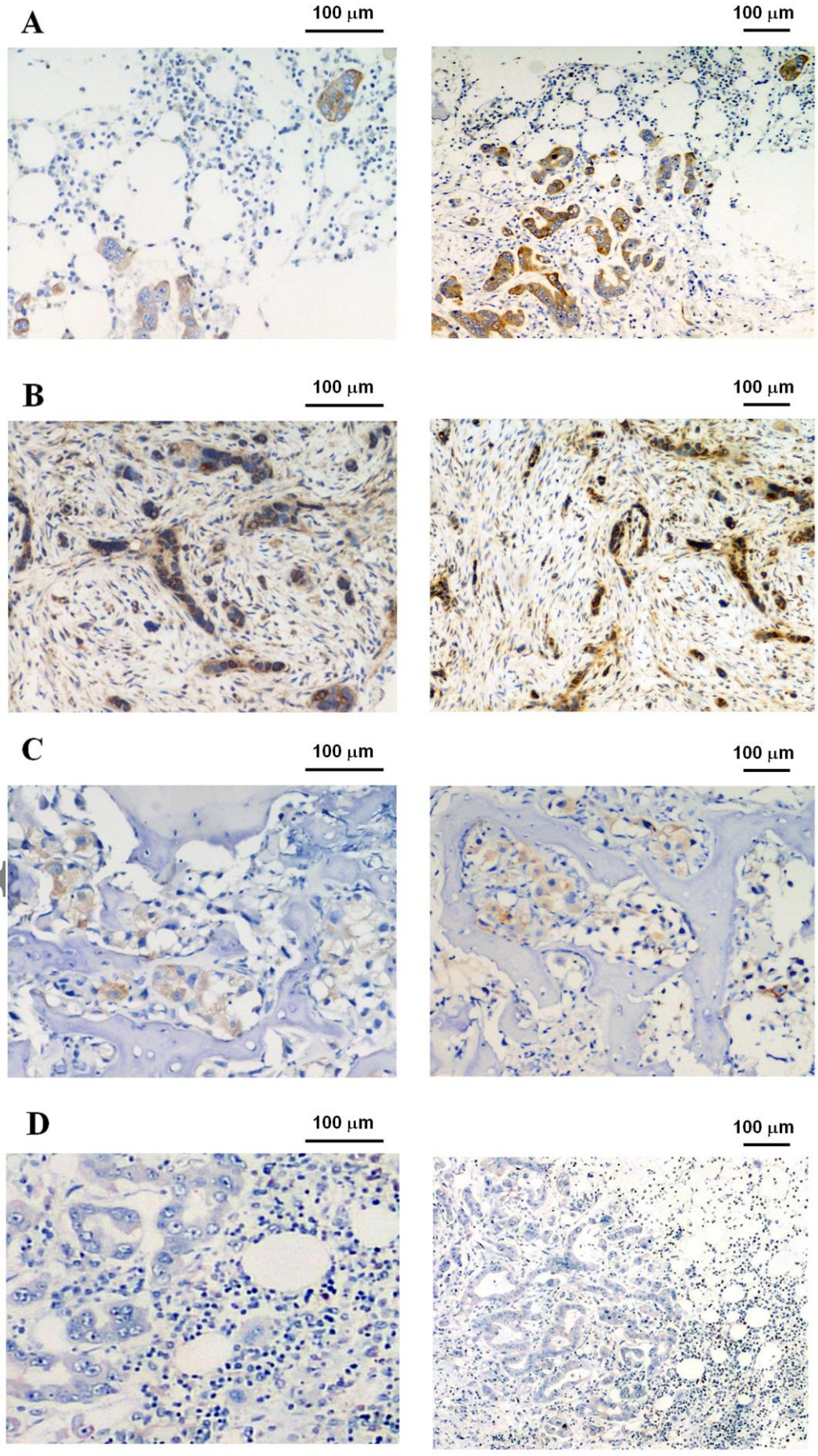

Fig. 3

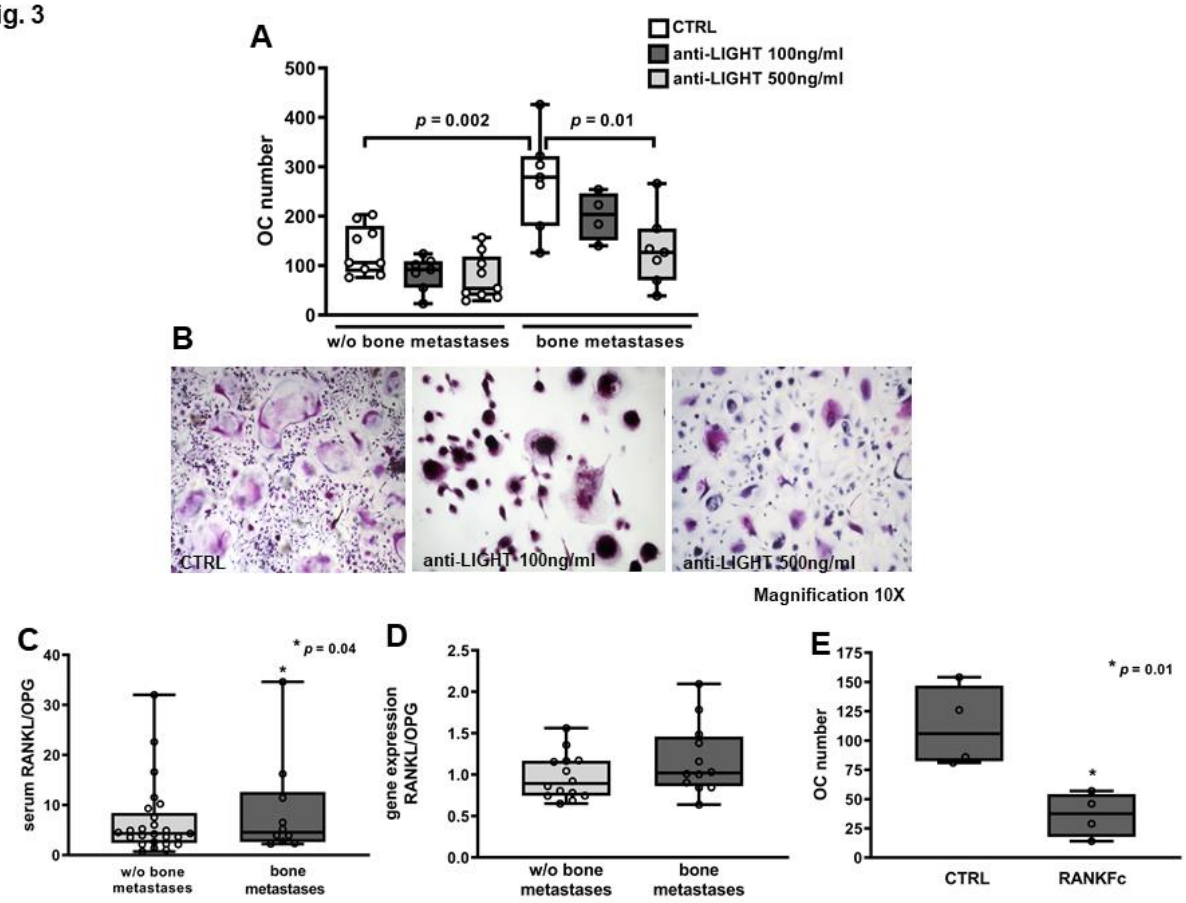

Fig. 4

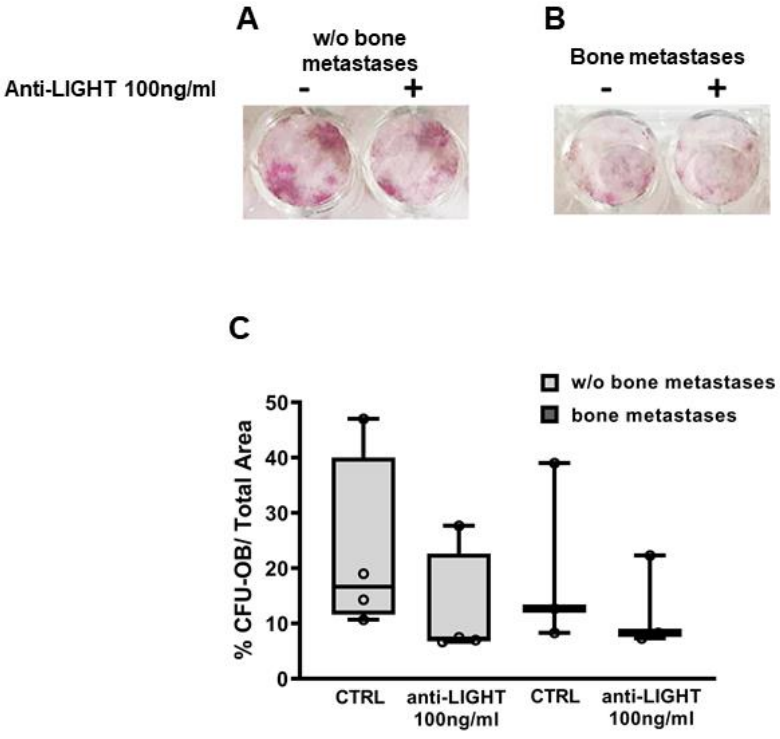

Figure 5

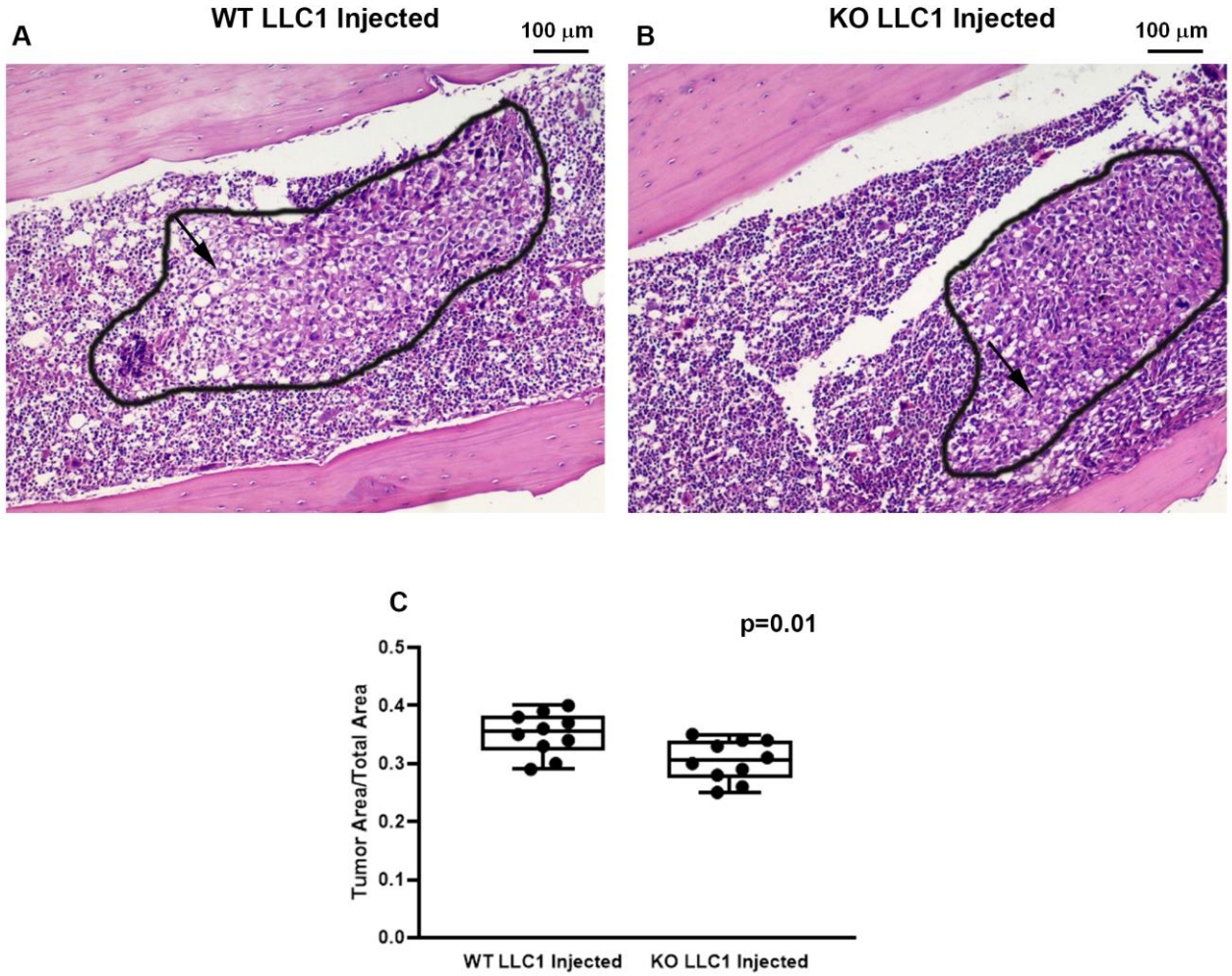

Fig. 6